Integrated climatology and trends in the subtropical Hadley cell, sunshine duration and cloud cover over South Africa

D. D. Mahlobo[1] T. Ndarana[2] S. Grab[1] F. Engelbrecht[1,3]

[1]School of Geography, Archaeology and Environmental Studies, University of the Witwatersrand, Johannesburg, South Africa

[2]Department of Geography, Geoinformatics and Meteorology, University of Pretoria, Pretoria, South Africa

[3]Council for Scientific and Industrial Research Natural Resources and the Environment, Pretoria, South Africa

Abstract

This study uses two methods to diagnose the local Hadley circulation; first the zonally averaged mass streamfunction, and second the stream function vector method. The two methods have been applied to the ERA-Interim reanalysis data for the period 1980-2015 to calculate both the climatology and trends of the Hadley cell. Both diagnostics advocate downwards mass flux being dominant over the subtropics, particularly over South Africa, yet the strength of Hadley cell is seasonal. Contrasts have been found between linear trends of the two diagnostics. Zonally symmetric diagnostics indicate strengthening of the Hadley cell, particularly in the subtropics of the Southern Hemisphere in winter and weakening in summer. The zonally asymmetric results indicate maximum strengthening of the Hadley cell over South Africa to be in spring and weakening in summer. Furthermore, maximum decrease in cloud cover and increase in sunshine duration over South Africa is in spring, implying more opportunities for solar energy generation.

KEYWORDS

Hadley circulation, mass flux, streamfunction, sunshine duration, total cloud cover

1 INTRODUCTION

The Hadley cell may be defined as a large-scale meridional circulation regime that is caused by differential heating at the earth's surface (e.g., Wallace and Hobbs, 2006). Unlike the Ferrell cell polewards of it, it is a thermally direct circulation that is characterized by ascending and descending branches in the tropical and subtropical regions, respectively. The convergence of warm air in the equatorial trough leads to uplift and polewards divergence in the upper troposphere and subsidence in the subtropics within the cell (under the influence of the Coriolis effect). The Hadley cell spans the tropical–subtropical belt in each hemisphere (Ceppi and Hartmann, 2013) and is the most prominent single circulation feature of the atmospheric circulation (Kang and Lu, 2012). The meridional extent of the Hadley cell characterizes the climates of the tropical and subtropical regions. On average, the air in the subsiding subtropical branch of the Hadley cell is dry and warm, which suppresses convective cloud formation.

As a consequence, the climates of subtropical land regions are largely arid to semi-arid, particularly on the west coast side of continents. The Hadley cell has been demonstrated to play an integral role in the context of anthropogenic-induced climate change and associated changes in the atmospheric circulation. Several studies have shown that the Hadley cell has progressively been widening (e.g., Johanson and Fu, 2009). Seidel and Randel (2007) demonstrated that increased frequency of higher subtropical tropopause heights and widening of the subtropical dry zones may have detrimental effects to precipitation and moisture budget in these regions. These changes have largely been attributed to increases in the concentrations of greenhouse gases (GHGs) in the atmosphere (Lu et al., 2007). During the austral summer months, ozone depletion has also played a role in augmenting the effects of GHGs (Polvani et al., 2011). It is expected that as GHG concentrations continue to increase into the future under various mitigation scenarios (Solomon et

al., 2007), the changes discussed above will persist. During the summer months, future widening will depend on the prevailing GHG scenario that actually materializes, with an opposing effect induced by ozone recovery (Polvani et al., 2011). For the strongly mitigated GHG scenario—Representative Concentration Pathway (RCP) 2.6-ozone recovery will overwhelm the impact of GHG's and widening will be reversed. With the RCP 8.5 (low mitigation) scenario, the effect of the GHGs will overwhelm that of ozone depletion, resulting in a continued widening of the Hadley cell (Johanson and Fu, 2009).

In addition to this meridional expansion, some studies have suggested that the descending branch is strengthening (e.g., Engelbrecht et al., 2009; Engelbrecht et al., 2011) and will continue to do so in future under low mitigation. This has been postulated as a key reason for the projected decrease in rainfall over southern Africa under low mitigation scenarios (Engelbrecht et al., 2009). Indeed, a widening and potential strengthening of the Hadley cell could lead to decreasing cloud cover and increasing sunshine or solar radiation over the subtropical land regions.

Clouds play an integral role in the earth's atmosphere and they involve a wide range of space and timescales (Bergman and Salby, 1997). They interact strongly with long wave and short wave radiation, which affects the distribution of surface and atmospheric heating. This in turn modulates atmospheric motions (Bergman and Salby, 1997). Through their characteristics and movement, clouds can also be seen as indicators of atmospheric motion as well as contributors to atmospheric and oceanic energetics (Warren et al., 1986). For this reason, the effects of cloud cover should not be separated from atmospheric circulation changes, as indicated above through potential changes in the Hadley cell. Cloud processes, including their interaction with atmospheric dynamics as well as their influence on the surface, must be understood clearly in order to understand climate regimes and circulation systems.

Solar radiation and sunshine duration at the earth's surface are impacted by cloud cover and could thus also be affected by changes in the Hadley circulation. The available solar energy at the

earth's surface is determined by surface net solar radiation and is a renewable energy resource (Kaggwa et al., 2011). The spatial and temporal distribution of solar radiation at the earth's surface under contemporary climate change is thus important to understand in order to assess climate change impacts on circulation and to understand impacts on the solar potential for renewable energy generation (e.g., Ruiz-Arias et al., 2011). According to Power and Mills (2004), South Africa has high climatological insolation values, receiving about 24 GWh/m2 per annum of solar radiation (Bugaje, 2006).

The topography of South Africa plays an important role in cloud cover and sunshine duration distribution (see Figure 1). The nine provinces of South Africa, Western Cape (WC), Eastern Cape (EC), Northern Cape (EC), North West (NW), Gauteng (GAU), Mpumalanga (MPU) and Limpopo are also shown in Figure 1. The western interior of South Africa receives more than 80% of possible annual sunshine. The eastern parts of South Africa receive a smaller percentage (50–60%) of possible annual sunshine due to greater cloud cover. The highest mean total radiation occurs during summer in the least cloudy western parts of the country (Tyson and Preston-Whyte, 2000; Kruger and Esterhuyse, 2005). Trends in cloud cover, solar radiation and sunshine duration for various regions have been documented in a number of studies (e.g., Liepert, 2002; Groisman et al., 2004; Wang and Key, 2005). A recent study (Singh and Kruger, 2017) on sunshine duration trends using point observations from 22 sunshine recording stations across South Africa identified a general decreasing trend for all seasons. However, the decrease was most prominently observed for the summer season. Over most parts of South Africa, Warren et al. (2007) found a decreasing trend in annual mean daily cloud cover. Kruger (2007) examined cloud cover trends over South Africa for the period 1960–2005 and found a decrease in both low and total cloud cover over much of the country. The extent of increasing cloud cover trends is greatest in spring and summer over the southern parts of South Africa.

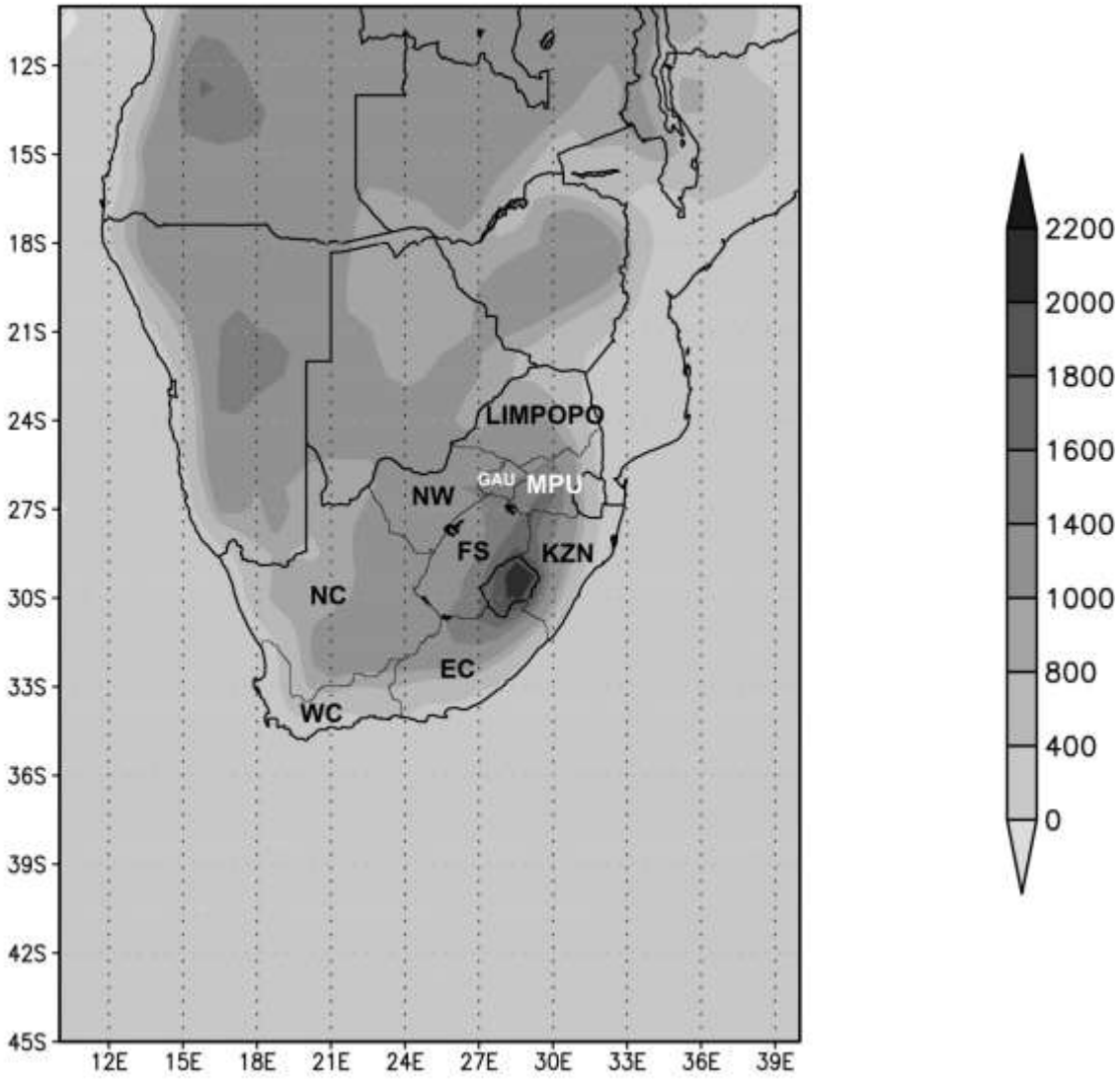

FIGURE 1 The provinces and topography of South Africa (altitude in meters above mean sea level)

The abundance in solar radiation and sunshine over South Africa is due to the fact that the country is located in the subtropical belt, exactly where the Hadley cell descending branch is located. However, it should be noted that solar radiation reaching the surface has a strong longitudinal gradient, which exists in relation to the longitudinal cloud cover (Loeb and Schuster, 2008), rainfall and sunshine duration. Against this background, it is important to determine how anthropogenic climate change may impact on the regional circulation, cloud cover and thus

rainfall and solar potential in South Africa. Whereas most studies of future climate change over southern Africa have focused on changes in the regional circulation and rainfall, the implications of changing cloud cover remains to be explored from a renewable energy perspective. Changes in the Hadley cell circulation would be key to understanding and anticipating the potential for such changes to occur. However, such a dynamic understanding and climatology of the Hadley circulation is missing for South Africa. Both zonally symmetric diagnosis, especially using the mass weighted stream function (Holton and Hakim, 2012), and zonally asymmetric (Schwendike et al., 2014; 2015) diagnosis, have focused more on the global scale.

However, first, an analysis of the Hadley cell, cloud cover and sunshine duration has not been undertaken to establish some form of relationship between the three variables using both zonally symmetric and zonally asymmetric diagnostics. Second, there has not been any regional study focussing on the Hadley cell in South Africa. Hence, this study aims to address this research gap by using the zonally symmetric diagnostics of the Hadley circulation to establish the climatology of zonally averaged Hadley cell, cloud cover and sunshine duration over subtropical regions of the Southern Hemisphere (SH). Furthermore, zonally asymmetric diagnostics will be used to construct the climatology as well as trends for the Hadley cell, cloud cover and sunshine duration.

2 DATA AND METHODS

2.1 Data

This study covers a 35-year period spanning from 1980 to 2015. Data for this study are based on the European Centre for Medium-Range Weather Forecasts (ECMWF) Interim Reanalysis (ERA-Interim). The ERA-Interim data set has been previously used by Nguyen et al. (2013), among other seven reanalysis data sets to diagnose the Hadley cell. All reanalysis data sets were in agreement with the climatology and variability of the Hadley cell. Hence, due to its fine

resolution, we use the ERA-Interim data set for our analysis. The data are on a horizontal resolution of 0.75^0x0.75^0 on 37 pressure levels (Dee et al., 2011). This horizontal resolution is considered sufficient to properly diagnose the dynamics of the descending branch of the Hadley circulation over South Africa. The vertical velocity at 500 hPa (which is the level that approximates maximum upwards vertical motion; Lu et al., 2007), meridional velocity from 1,000 to 10 hPa levels, total cloud cover and sunshine duration were used to construct climatologies and linear trends of the Hadley cell, total cloud cover and sunshine duration. Additional data to analyse the climatology and trends of cloud cover and sunshine hours, was obtained from the South African Weather Service (SAWS).

Only stations with continuous data for the period 1980-2015 were used in the analysis, and these made up a total of 24 stations with cloud cover and 17 stations with sunshine hours. SAWS cloud cover and sunshine hours observations are made in accordance with World Meteorological Organisation (WMO) standards. Cloud cover trends over South Africa for the period 1960 to 2005 were constructed by Kruger (2007) using observational data from SAWS. In this study, an update of cloud cover trends is presented using both ERA-Interim and SAWS observations.

2.2 Methods

2.2.1 Zonally averaged mass streamfunction

To quantify changes of the Hadley cell, we use the zonally symmetric diagnosis, which have been used in a number of studies (e.g., Johanson and Fu, 2009; Polvani et al., 2011; Nguyen et al., 2013). The Hadley circulation is described as a large-scale meridional overturning of a rotating atmosphere and is characterized by maximum heating at the surface close to the equator. The strength and structure of the Hadley cell can be quantified using the zonally averaged stream

function, given by the motivation outlined in Appendix A. The resulting stream function expression that will be used is given by (Polvani et al., 2011),

$$\Psi(\phi, p) = \frac{2\pi a cos\phi}{g} \int_{P}^{P_1} \bar{v} dp' \qquad (1)$$

where ϕ is latitude, p pressure, $\bar{v}$ the zonal mean meridional wind, a the radius of the earth and g the gravitational acceleration.

We note that ψ describes the meridional circulation in general (i.e., both direct and in direct cells). To distinguish between these cells, Holton and Hakim (2012) show that

$$\Psi \propto -\frac{\partial \bar{J}}{\partial y} + \frac{\partial^2}{\partial^2 y}(\overline{vT'}) + \frac{\partial^2}{\partial y \partial z}(\overline{u'v'}) + \frac{\partial}{\partial z}(zonal\ drag) \qquad (2)$$

where y and z represent the northwards and upwards directions, respectively, u', v' and T' are the perturbations of the eastwards component of the wind, northwards component of wind as well as the temperature, respectively. This decomposition of ψ demonstrated that diabatic heating ($\bar{J}$), large-scale eddy processes viz large-scale eddy heat fluxes ($\overline{v'T'}$) and momentum fluxes ($\overline{u'v'}$) and friction play a role in determining which aspect of ψ applies to which aspect of the meridional circulation (the Hadley circulation, the Ferrel cell or the polar cells).

A positive meridional temperature gradient occurs in the SH, implying that the aspect of ψ in Equation (2) associated with diabatic heating, will thus be negative there. The first term is associated with the thermally direct circulation. This means that $\psi < 0$ represents the Hadley cell in the SH.

To define the strength of the Hadley cell, we use the maximum value of meridional mass stream function averaged between 900 and 200 hPa (Nguyen et al., 2013), but take the possible expansion of the cell by dividing values by the difference in latitude (i.e., $\psi_{max}/(\varphi_{max} - \varphi_{edge})$),

where φ_{max} and φ_{edge} are the latitudes where is maximum and at the edge of the cell. This edge is defined first by determining the maximum meridional mass stream function at 500 hPa, and the edges are then determined by taking the first latitude polewards of the maximum at which $\psi = 0$ (Lu et al., 2007).

2.2.2 Diagnostics for the local Hadley circulation

Schwendike et al. (2014) showed that it is possible to decompose Equation (A1) in such a way that continuity is satisfied independently in both the zonal and meridional direction, using a variation of the vector method (Keyser et al., 1989). The continuity equations in the zonal and meridional directions are, respectively, given by

$$\frac{1\partial u}{a\partial\lambda} + \frac{\partial}{\partial p}(\omega_\lambda cos\phi) = 0, \qquad (3a)$$

$$\frac{1\partial}{a\partial\phi}(vcos\phi) + \frac{\partial}{\partial p}\left(\omega_\phi cos\phi\right) = 0, \qquad (3b)$$

where $\omega = \omega_\lambda + \omega_\phi$ is the sum of the vertical motion, partitioned into zonal and meridional directions, as indicated by the subscripts λ and ϕ, respectively. Note that an outline of the derivation of this partitioning of Equation (A1) is given in Appendix B.

Equations (3a) and (3b) operate on orthogonal vertical zonal and meridional planes, respectively. In particular, (v, ω_ϕ) represents the overturning circulation on the vertical meridional plane, which when confined to the tropics and subtropics, uniquely diagnoses the Hadley circulation. Following Schwendike et al. (2014), the upwards vertical flux of mass in this circulation is represented by $m_\phi = (\omega_\phi cos\phi)\ g^{-1}$.

Given the vertical motion ω obtained from the ERA-Interim data set, we calculate the potential function μ by solving the Poisson's Equation (B3) using the HWSSSP subroutine of the National Centre for Atmospheric Research (NCAR) Software Library (Swarztrauber, 1974), which is written in FORTRAN 77, as in D'Abreton and Tyson (1995). From the resulting μ field, the ψ vector stream function components are calculated using Equation (B4) from which the vertical mass flux m_ϕ is then calculated. Linear trends of the Hadley diagnostics, sunshine hours and total cloud cover from the ERA-Interim for the four seasons were constructed. The Student's t test was used to test trends for statistical significance at the 95% level.

3 RESULTS AND DISCUSSION

3.1 Climatology of zonally symmetric diagnostics: Streamfunction, sunshine duration and total cloud cover

Several previous studies (e.g., Johanson and Fu, 2009; Polvani et al., 2011; Kang and Lu, 2012; Nguyen et al., 2013) have addressed the variability and changes in the Hadley circulation; here we consider possible implications of these changes to cloud cover and sunshine hours. While it is difficult to make conclusions of a regional nature from zonally averaged diagnostics, they serve as a prelude to the zonally asymmetric discussion; we therefore consider these issues from the former first.

Fig. 2 shows the seasonal variations of the in 10^9 $kg.s^{-1}$. The negative values indicate anticlockwise motion, with the contours south of the central axis (represented by the thick red contour) which goes through the maximum value of showing areas of subsidence south of it, according to (A4). Similarly, the negative values of north of the central axis represent regions of ascent. As the region of interest is southern Africa, we therefore consider these variables between 50^0S and 5^0N.

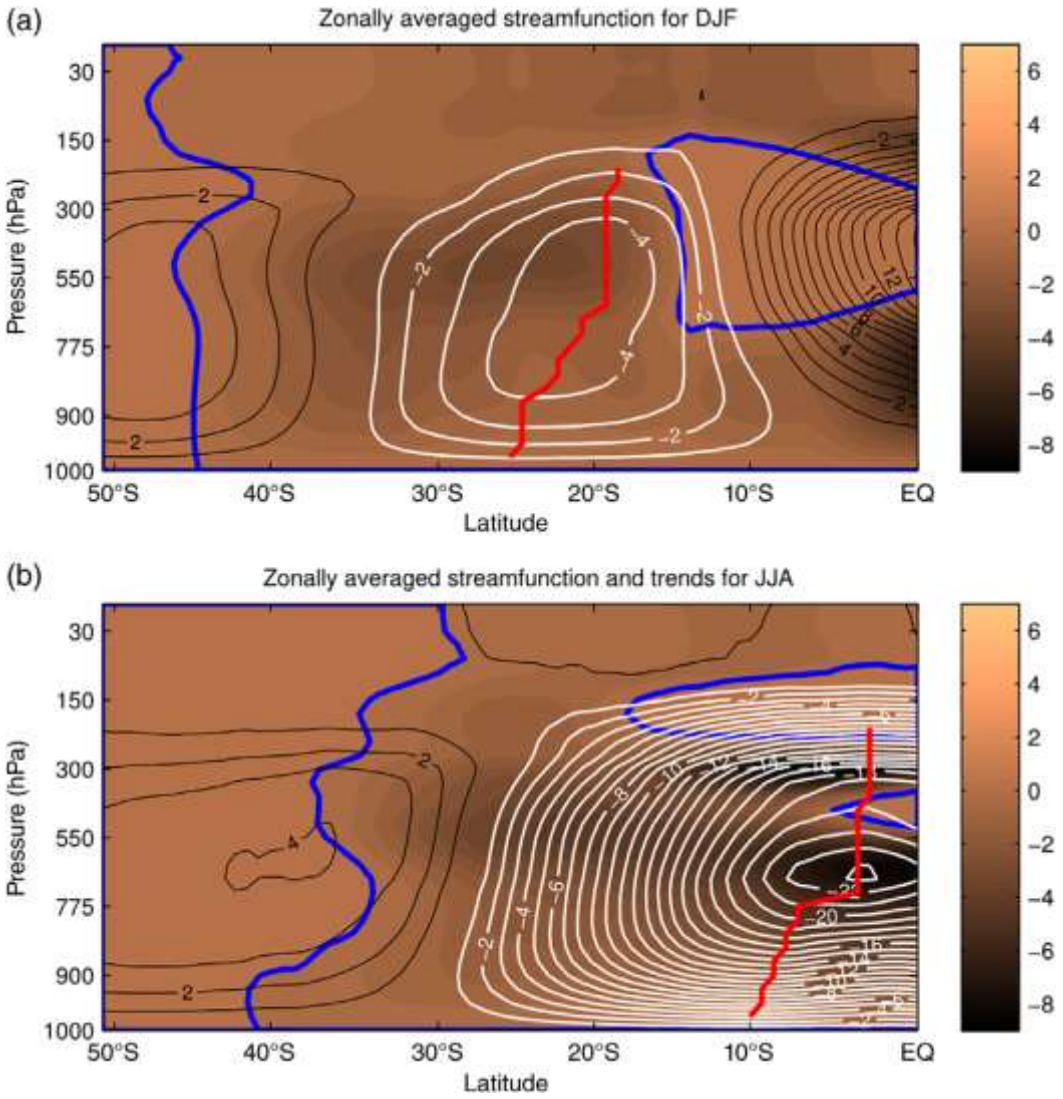

FIGURE 2 Climatology of zonally averaged negative (thin black contours) and positive (thin white contours) streamfunction and associated trends (shaded) for (a) DJF and (b) JJA. The thick blue contours represent regions where the zonally averaged streamfunction is zero and the thick red contours represent regions where the trends turn from negative (lighter shade) to positive (darker shade).

A strong seasonal dependence, as well as intensity of the circulation, is evident (Figure 2 and Table 1). Subsidence over austral subtropics is noted during all seasons, which is weakest during December–February (DJF) (Figure 2a) but strongest from June to August (JJA) (Figure 2b). The strength of subsidence during the solstice seasons appear to be comparable, which suggests that these are transition seasons between the DJF minimum and JJA maximum strengths. The

variations in strength are indicated by the meridional gradient, as implied by Equation (A4). Tighter (higher) gradients induce stronger flow. The ascending branch of the circulation exhibits exactly the same behaviour. A similar argument about the meridional flow can be made based on differences in the vertical gradients of Equation (A3). Again, these gradients reach minimum and maximum values during DJF and JJA, respectively (Table 1). The intensity of the Hadley circulation reaches minimum (i.e. -8.97 $x10^6$ kg s^{-1} km^{-1}) and maximum (i.e. -38.5 $x10^6$ kg s^{-1} km^{-1}) values during DJF and JJA, respectively.

TABLE 1 The Hadley cell Intensity climatology (10^6 kg s^{-1} km^{-1}), trends (10^4 kg $s^{-1}km^{-1}$) and the climatology for the Hadley cell edge (degrees of latitude) for DJF, MAM, JJA and SON

	Hadley cell intensity climatology	**Hadley cell intensity trends**	**Hadley cell edge latitude**
DJF	-8.97	-9.6	-36
MAM	-20.1	4.85	-33
JJA	-38.5	5.46	-28
SON	-21.2	0.02	-30

There are significant seasonal variations in the position of the Hadley circulation (Figure 2). During austral winter, the circulation appears to migrate northwards. This migration is clearly evident in Table 1 (column 3), where the edge is at its southern (northern) most position during DJF (JJA) at 36^0S (28^0S). The Asian summer monsoons and displacement of the ITCZ are the main contributors of the meridional shift of the circulation. In fact there is a strong link between the migration of the Hadley cell edges of the Hadley cell and the ITCZ (Kang and Lu, 2012).

The seasonal variations of cloud cover as a percentage of total sky, and sunshine hours are represented as a dashed line in Figures 3 and 4, for DJF and JJA, respectively. The seasonal variability of total cloud cover is broadly consistent with that of the Hadley circulation (compare

Figures 2, 3a and 4a for the corresponding seasons). Where there is descending motion in the subtropical regions, less total cloud is found, compared to regions where rising motion of air is found. This is not unexpected, of course, because tropical air is expected to be moist and warm,

while the descending branch in the subtropics is characterized by air that is dry as it adiabatically warms. The subtropical dry zones migrate northwards from DJF to JJA, which is consistent with the variability of rainfall over South Africa (Tyson and Preston-Whyte, 2000). This part of the SH receives most of its rainfall during the summer months, when the Hadley circulation is at its weakest.

Figure 2 shows the seasonal variations of the ψ in 10^9 kg/s. The negative values indicate anticlockwise motion, with the contours south of the central axis (represented by the thick red contour) which goes through the maximum value of ψ showing areas of subsidence south of it, according to Equation (A4).

Similarly, the negative values of ψ north of the central axis represent regions of ascent. As the region of interest is southern Africa, we therefore consider these variables between 50S and 50N. A strong seasonal dependence, as well as intensity of the circulation, is evident (Figure 2 and Table 1). Subsidence over austral subtropics is noted during all seasons, which is weakest during December–February (DJF) (Figure 2a) but strongest from June to August (JJA) (Figure 2b). The strength of subsidence during the solstice seasons appear to be comparable, which suggests that these are transition seasons between the DJF minimum and JJA maximum strengths. The variations in strength are indicated by the meridional gradient, as implied by Equation (A4). Tighter (higher) gradients induce stronger flow. The ascending branch of the circulation exhibits exactly the same behaviour. A similar argument about the meridional flow can be made based on differences in the vertical gradients of Equation (A3). Again, these gradients reach minimum and maximum values during DJF and JJA, respectively (Table 1). The intensity of the Hadley

circulation reaches minimum (i.e., -8.97×10^6 kg s^{-1} km^{-1}) and maximum (i.e., -38.5×10^6 kg s^{-1} km^{-1}) values during DJF and JJA, respectively.

There are significant seasonal variations in the position of the Hadley circulation (Figure 2). During austral winter, the circulation appears to migrate northwards. This migration is clearly evident in Table 1 (column 3), where the edge is at its southern (northern) most position during DJF (JJA) at 36^0S (28^0S). The Asian summer monsoons and displacement of the ITCZ are the main contributors of the meridional shift of the circulation. In fact there is a strong link between the migration of the Hadley cell edges of the Hadley cell and the ITCZ (Kang and Lu, 2012).

The seasonal variations of cloud cover as a percentage of total sky, and sunshine hours are represented as a dashed line in Figures 3 and 4, for DJF and JJA, respectively. The seasonal variability of total cloud cover is broadly consistent with that of the Hadley circulation (compare Figures 2–3a and 4a for the corresponding seasons). Where there is descending motion in the subtropical regions, less total cloud is found, compared to regions where rising motion of air is found. This is not unexpected, of course, because tropical air is expected to be moist and warm, while the descending branch in the subtropics is characterized by air that is dry as it adiabatically warms. The subtropical dry zones migrate northwards from DJF to JJA, which is consistent with the variability of rainfall over South Africa (Tyson and Preston-Whyte, 2000). This part of the SH receives most of its rainfall during the summer months, when the Hadley circulation is at its weakest.

3.2 Trends in streamfunction, total cloud cover and sunshine duration

Linear trends of the zonally averaged Hadley cell at 500 hPa level for DJF and JJA for the period 1980–2015 are shown in Figure 2, the Hadley cell intensity trends are also shown in Table 1. The

positive Hadley cell intensity index indicates an increase in upwards mass streamfunction (downwards mass streamfunction) over the tropics (subtropics) and vice versa. A decrease in the upwards mass streamfunction is evident over areas of positive meridional mass streamfunction and subsequently a decrease in the downwards mass streamfunction over the SH subtropical zones in DJF. The general decrease in downwards motion in the subtropical Hadley cell is evidenced by the Hadley cell intensity index of 9.76×10^4.

The maximum rate of increase in downwards motion is found in JJA and the Hadley cell index is -5.46×10^4. The linear trends of the meridional mass streamfunction also indicate a polewards shift of the Hadley cell (i.e., the Hadley cell edges are located further polewards than in the climatology and this is consistent with previous studies) (Johanson and Fu, 2009). The southwards expansion and intensification of the cell, which also manifests as an increase in the subtropical dry zones (Seidel and Randel, 2007), is evident in all seasons except for DJF.

Lu et al. (2007) found that the expansion of the Hadley cell is positively correlated with an increase in greenhouse gases (GHGs), while Garfinkel et al. (2015) attribute the expansion of the Hadley cell to GHGs, stratospheric ozone depletion, tropospheric ozone and SSTs. Stratospheric ozone depletion is the more dominant driver of tropospheric changes such as the expansion of the Hadley circulation and the polewards shift of the eddy-driven jet (Polvani et al., 2011). The increase in subtropical zones could mean the spatial extent of cloudlessness and more sunshine hours has also increased, as is consistently found in this study. This is in agreement with Tselioudis et al. (2016), who further pointed out that the expansion of the Hadley cell is linked to the polewards shift of mid-latitude clouds. This polewards shift enables more sunlight to reach the surface and hence leads to surface radiative warming.

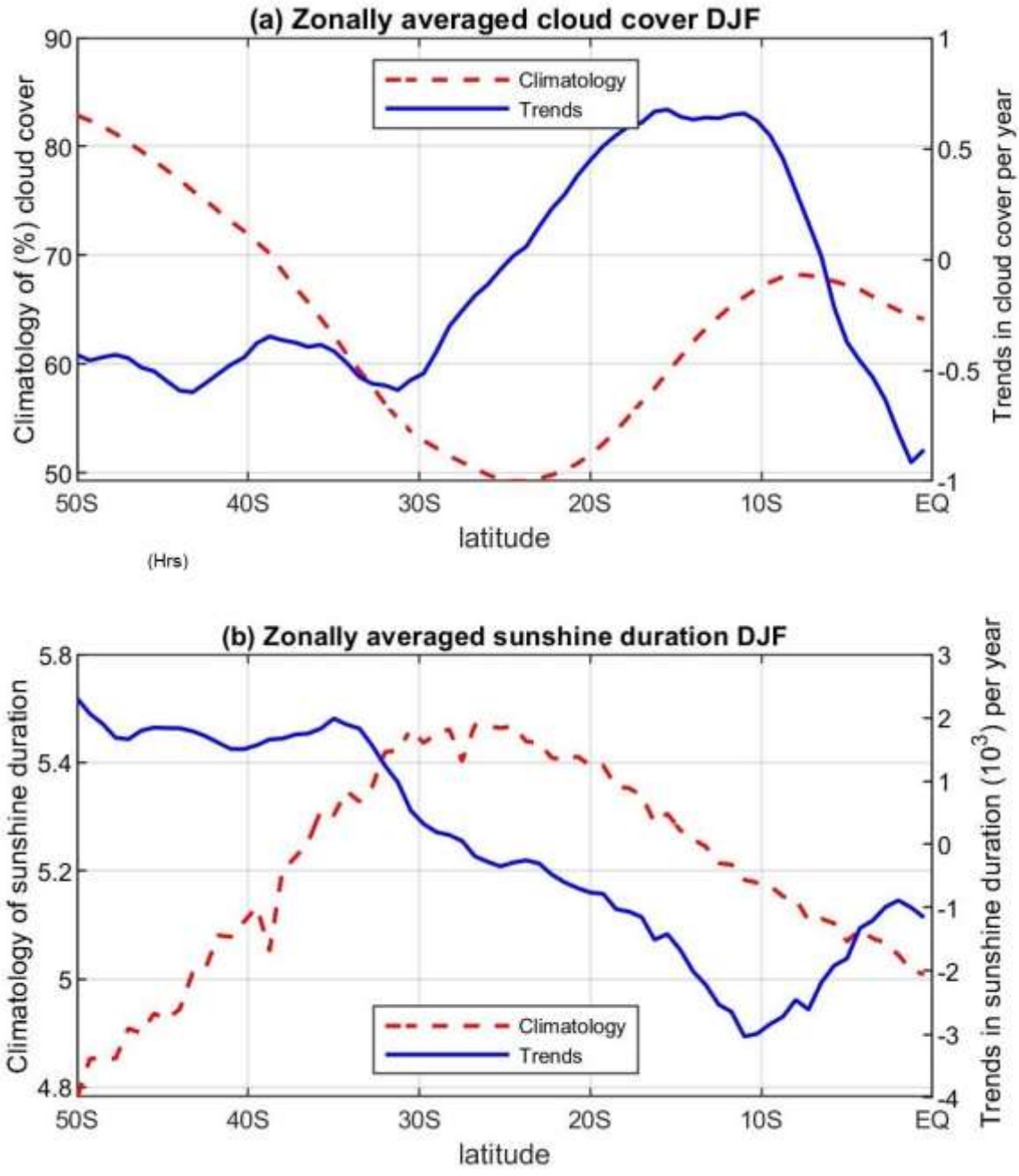

FIGURE 3 (a) The climatology (dashed line) and trends (solid line) of zonally averaged cloud cover for DJF. (b) Same as (a) but for zonally averaged sunshine duration (sunshine hours per day)

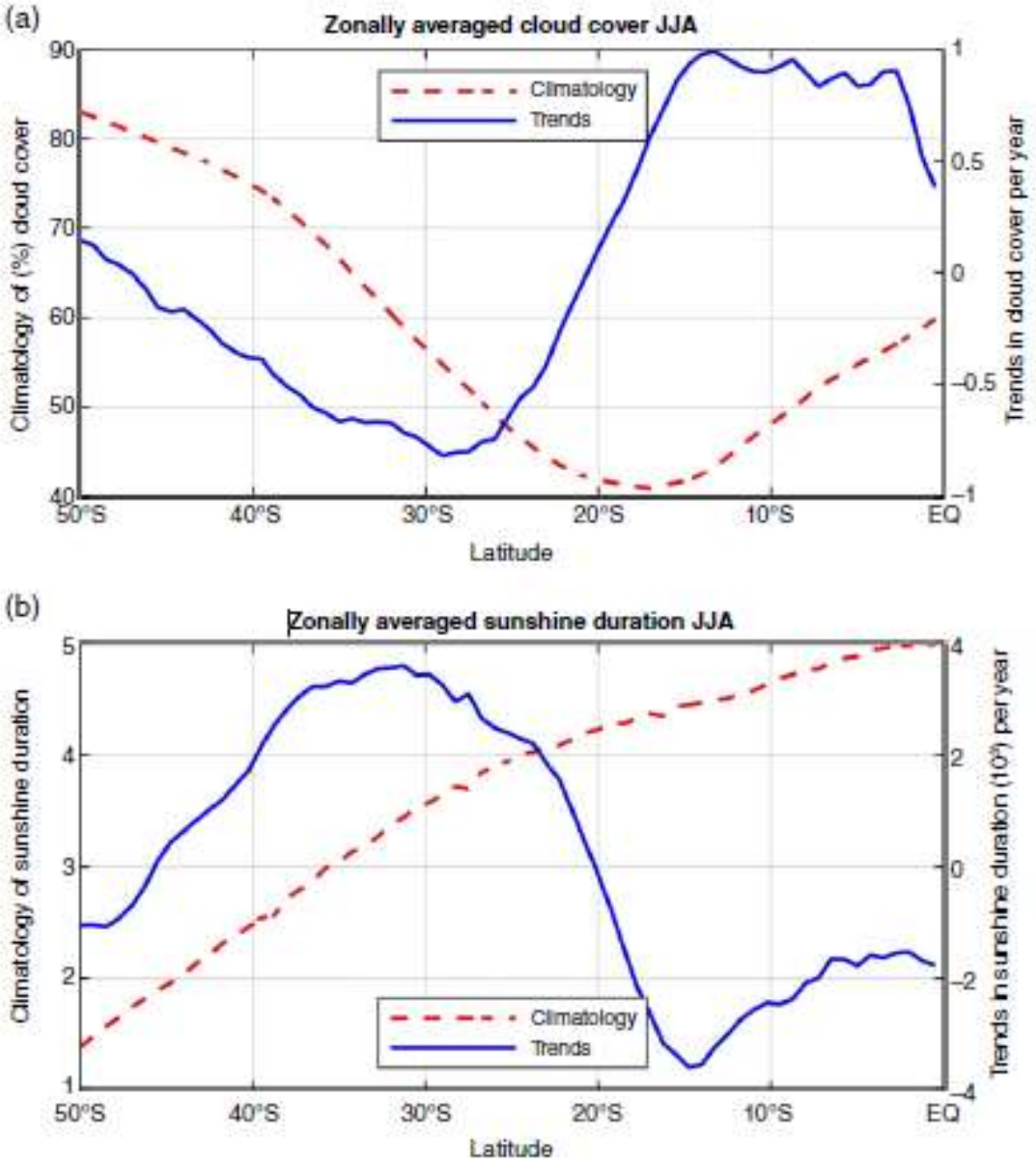

FIGURE 4 (a) The climatology (dashed line) and trends (solid line) of zonally averaged cloud cover for JJA. (b) Same as (a) but for zonally averaged sunshine duration

The linear trends of total cloud cover and sunshine duration over the descending branch of the Hadley cell are shown in Figures 3 and 4 for DJF and JJA, respectively. An increase in total cloud cover is evident from the equator to latitude 20^0S in JJA and a decrease from latitude 20^0S to further southwards, but in DJF (Figure 3a) a decrease is evident from the equator to about 7^0S and from 24^0S to further southwards. The rate of increase (tropics) and decrease (subtropics) is more

in JJA and less in DJF. This is consistent with the Hadley cell intensification in JJA and weakening in DJF. Similar to the meridional mass stream function and zonally averaged cloud cover trends, linear trends in zonally averaged sunshine duration are also seasonal. A decrease in sunshine duration from the equator to the subtropics (around latitude 29^0S) is evident in DJF (Figure 3b); however, in JJA (Figure 4b) a decrease in sunshine duration is evident from the equator to latitude 19^0S, thereafter an increase is evident for all lower latitudes. A clear correspondence between trends over the different latitudes compares well with results from Singh and Kruger (2017), for example, positive trend in sunshine duration south of 30^0S but turning negative northwards in DJF and negative trends south of 30^0S in JJA.

The combined trend analysis between the zonally averaged Hadley, total cloud cover and sunshine hours over the subtropics, is broadly consistent. In JJA the descending motion resulting from the negative gradient of the stream function is consistent with a decrease in total cloud cover and an increase in sunshine hours over the descending branch of the Hadley. Over the tropics (SH), an increase in upwards vertical motion (positive meridional mass stream function), increase in total cloud cover and decrease in sunshine hours is mostly evident in JJA.

In summary, the subtropical branch of the Hadley cell has intensified and expanded southwards in JJA (with negative values of the meridional stream function becoming more negative), which is consistent with other studies (Engelbrecht et al., 2011). Also in JJA, total cloud cover has decreased and sunshine duration has increased over the subtropics of the SH and both have shifted polewards. A quantitative correlation of the Hadley intensity, total cloud cover, as well as the sunshine duration over the subtropics of the SH, has also been performed for all seasons (Table 2). Only weak correlations are established for all the seasons. It is likely that zonal averaging may have compromised the correlation between the zonally averaged mass stream function and zonally averaged cloud cover and sunshine duration.

TABLE 2 Correlation coefficients between the Hadley cell intensity (HCI), zonally averaged total cloud cover (TCC) and zonally averaged sunshine duration (SunD) for DJF, MAM, JJA and SON.

	Correlation HCI and TCC	**Correlation HCI and SunD**	**Correlation SunD and TCC**
DJF	-0.4	0.27	-0.8
MAM	-0.15	0.03	-0.73
JJA	-0.29	0.19	-0.79
SON	-0.35	0.23	-0.75

These results are further perpetuated when examining regional changes of the Hadley, in particular over South Africa, which in some way contributes to the intensification and expansion of the subtropical Hadley. Since these diagnoses were based on zonally averaged data, some of the regional features that may contribute to the expansion may be missed. A possible way of investigating regional changes is through zonally asymmetric methods.

3.3 Climatology of zonally asymmetric diagnosis

The local Hadley cell over South Africa, as defined by the meridional mass flux at 500 hPa, is characterized by the general decent of vertical motion in all seasons (Figure 5a,d), which is typical of subtropical weather. Consequently, the subtropics are characterized by semi-permanent anticyclones which are caused by large-scale subsidence on the descending branch of the Hadley cell. These anticyclones are a large contributing factor to the weather of South Africa (Tyson and Preston-Whyte, 2000), such as when they ridge and bring moisture over the eastern parts of the country. The mean vertical motion over South Africa is downwards, however the strength of this motion is seasonal and vertical motion occurs at times, as the number of anticyclones decreases (Tyson and Preston-Whyte, 2000). When upwards vertical motion occurs, it is confined to where weather systems such as cut-off lows (COLs; e.g., Engelbrecht and Landman, 2014) and tropical-

temperate troughs (TTTs; e.g., Hart et al., 2010) occur and elsewhere subsidence dominates (Tyson and Preston-Whyte, 2000). This is shown by the grey dots over the interior of the country, south of the northern thick contour in Figure 5. The southern and western parts of the country experiences maximum subsidence and this is consistent with ridging Atlantic anticylones (Tyson and Preston-Whyte, 2000).

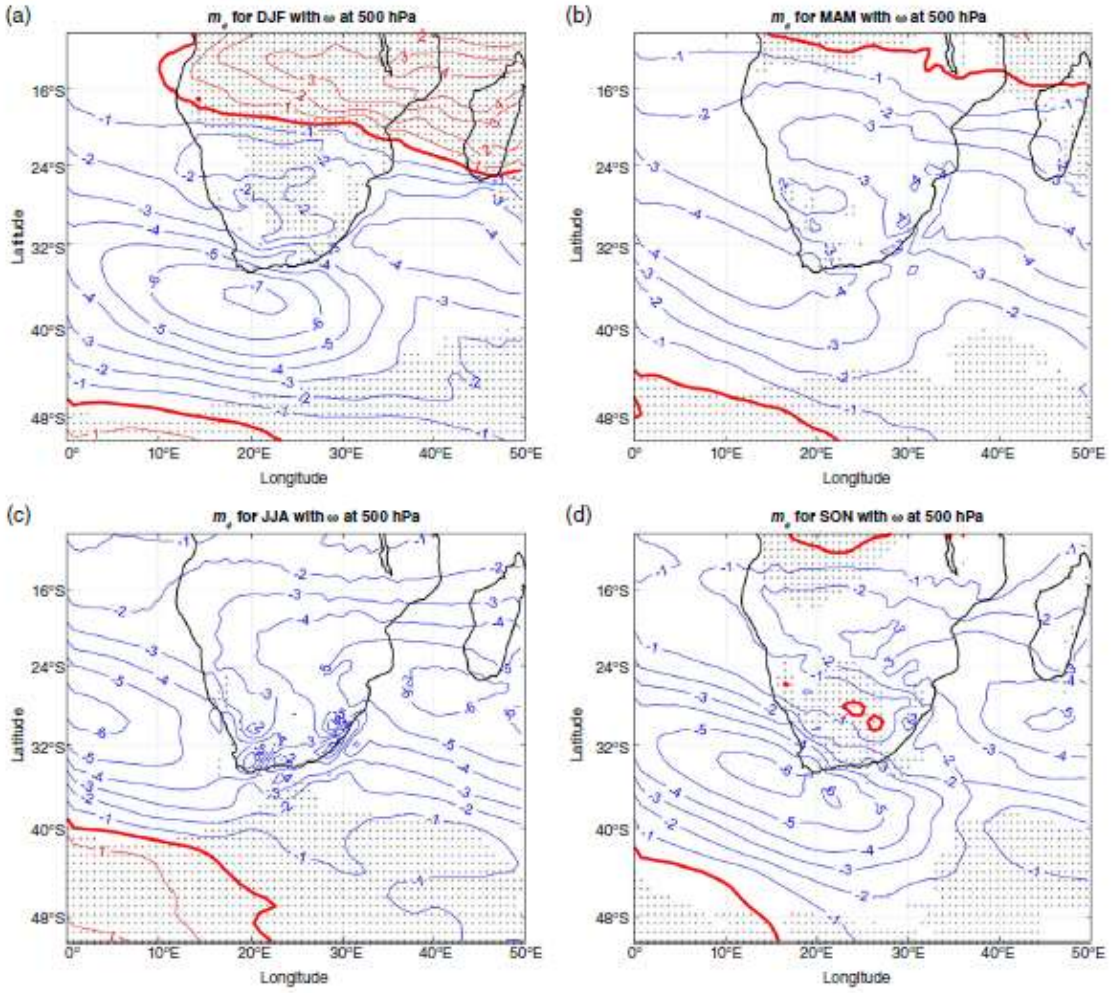

FIGURE 5 Seasonal mean of the mass flux (m_φ) and the units are kgm^{-2}/s and vertical velocity (ω) in Pa/s for (a) DJF, (b) MAM, (c) JJA and (d) SON. Values of the mass flux are represented by thin contours. The thick contours represent regions where the mass flux is zero. The contours are plotted in 10^3 kgm^{-2}/s intervals. Regions of upwards vertical velocity is represented using the grey dots and where there are no grey dots then there is downwards motion there (i.e., $\omega > 0$)

The weaker Hadley circulation over the country that is evident in DJF (Figure 5a) and September–November (SON; Figure 5d) may also be linked to the frequency of anticyclones. In DJF the number of anticyclones decreases and the circulation over South Africa is dominated by a weak heat low that is joined by a trough across the Northern Cape to a tropical low north of Botswana (Tyson and Preston-Whyte, 2000). The centre of the low is fashioned in an east–west direction along the southern branch of the ITCZ in the Congo Air Boundary and seldom southwards towards Namibia and Botswana. East of the trough or low, upwards vertical motion exists (Tyson and Preston-Whyte, 2000), resulting in the reduction of the Hadley cell subsidence over the summer rainfall region. This is advocated by the low values of subsidence over interior of South Africa. Lowest values are confined to the far northern parts of Limpopo Province, far northern parts of North West Province and further southwards to Free State Province. Warming of the surface in the austral summer also plays a role in the seasonal strength of the subtropical Hadley cell. Land surface warming affects the meridional temperature gradients that weaken subsidence during summer months (Cook, 2003). It is also warming of the surface that causes convection at the surface, leading to thunderstorm development (Tyson and Preston-Whyte, 2000). Vertical ascent due to thunderstorms and other weather systems which are prevalent over South Africa during summer suppress the descending motion of the Hadley cell, making it weaker.

In JJA, maximum subsidence is evident throughout the country with higher values of negative mass flux confined to the summer rainfall region of South Africa and less negative mass flux values over the all year rainfall region (Figure 5c). Surprisingly, the south western parts of South Africa also show highest values of the subsidence. The downwards mass flux over the Western Cape should be lower because this is a winter rainfall region (as also shown by the upwards vertical motion there). The austral winter experiences the maximum frequency of anticyclones (Tyson and Preston-Whyte, 2000). These anticyclones are more intense during this season.

They migrate northwards and are located over the interior of South Africa replacing the surface trough. Simultaneously, the upper-level westerlies widen and the upper tropical easterlies are displaced northwards, resulting in maximum subsidence over South Africa. This leads to subsidence throughout the country, confirming the descent in JJA, with exceptions of the South Western Cape (as noted above) and southern parts where weather is dominated by frontal systems (Tyson and Preston-Whyte, 2000). The subsidence is greatly linked to high atmospheric stability and subsidence inversion. The surface inversions suppress convection and dispersion of pollutants. These inversions restrict the extent of meridional temperature gradients due to surface cooling in winter, leading to more subsidence and thus a stronger subsidence in the Hadley circulation.

As was the case with the zonally averaged diagnostics, the solstice seasons exhibit transitional behaviour of the Hadley circulation, in both strength and movement. This and the discussion above shows that the zonally varying Hadley circulation migrates northwards from DJF to JJA. However, the contradiction is that the descending motion appears to be stronger during summer in this case, south of the African continent. This highlights the importance of using locally varying diagnostics as these enable local meteorology to be taken into consideration.

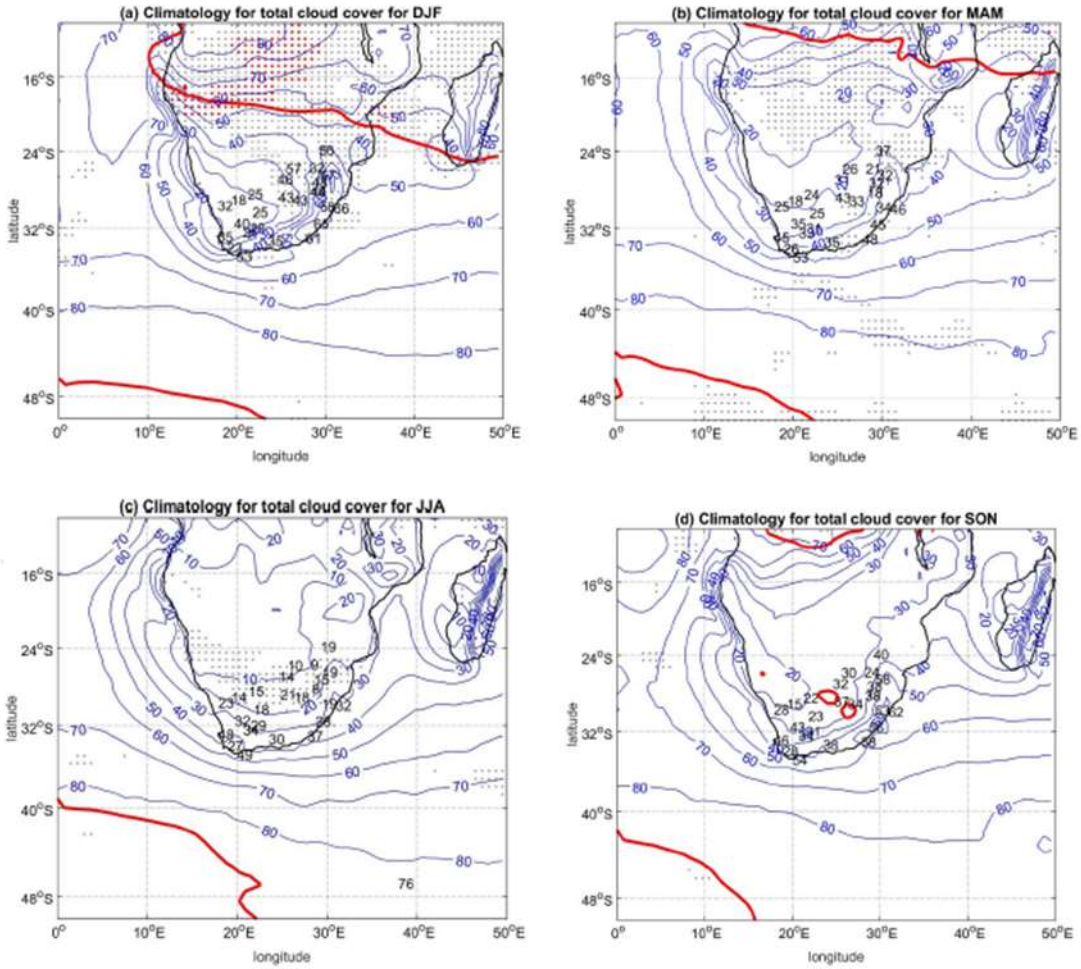

FIGURE 6 Total cloud area fraction shown as a percentage for (a) DJF, (b) MAM, (c) JJA and (d) SON is presented as thin contours (from the ERA-Interim) and the values in black (for each SAWS station observation used in the analyses). Regions where the mass flux is zero are presented as thick contours. Correlations between total cloud cover and mass flux of Figure 5 are represented as dots. Only positive correlations are shown, grey dots are correlations between zero and 0.5 and where there are no dots, cloud cover and mass flux are negatively correlated

The seasonal climatology of total cloud cover is shown in Figure 6. Correlation greater than 0.5 is established only in DJF but found only north of South Africa from latitude 22^0S northwards. Weak correlation (between 0 and 0.5) is also found north of South Africa in DJF and SON, and no

correlation was established in South Africa. One noticeable feature about the correlation is that although weak, it is only found in JJA over the central interior of South Africa, exactly where the Hadley cell and the subsequent subsidence are dominant. This could mean that cloud cover over South Africa, does not entirely depend on the Hadley cell but depends more on weather producing systems that dominate the country, and particularly in summer.

The climatology of cloud cover and sunshine duration informed by the ECMWF data is represented in contours and the bold values represent each SAWS station used in the analyses and the climatology of cloud cover for that particular station (Figures 6 and 7). Although there are some inconsistencies spatially, cloud cover from both the SAWS station data and ECMWF data indicate high cloud cover values over the eastern parts of South Africa; these values decrease as one moves westwards. South African coasts also receive less sunshine and more cloud cover; however, over the west coast, less cloud cover can be attributed to the persistent radiation fog that occurs over this region (Kruger and Esterhuyse, 2005).

Although all seasons follow the above overview of sunshine duration and cloud cover, there are significant seasonal variations. The western parts appear to have more or less consistent sunshine and cloud cover in all seasons, whereas the eastern parts possess more variations in terms of sunshine duration and cloud cover in the four seasons. This may be due to different circulations that occur over southern Africa. These circulation types are linked to cloud bands that define widespread cloud cover over South Africa. In DJF maximum cloud cover is experienced over most of South Africa but to a larger extent over the eastern parts of the country (Figure 6a). This could be attributed to major cloud bands over South Africa. Major cloud bands account for most of South Africa's annual rainfall; they occur together with TTTs and are frequent in South Africa during austral summer (Tyson and Preston-Whyte, 2000).

From March to May (MAM) and September to November SON (Figure 6b, d), relatively lower values of cloud cover are evident over South Africa; the eastern parts exhibit higher values and the western parts indicate lower cloud cover values.

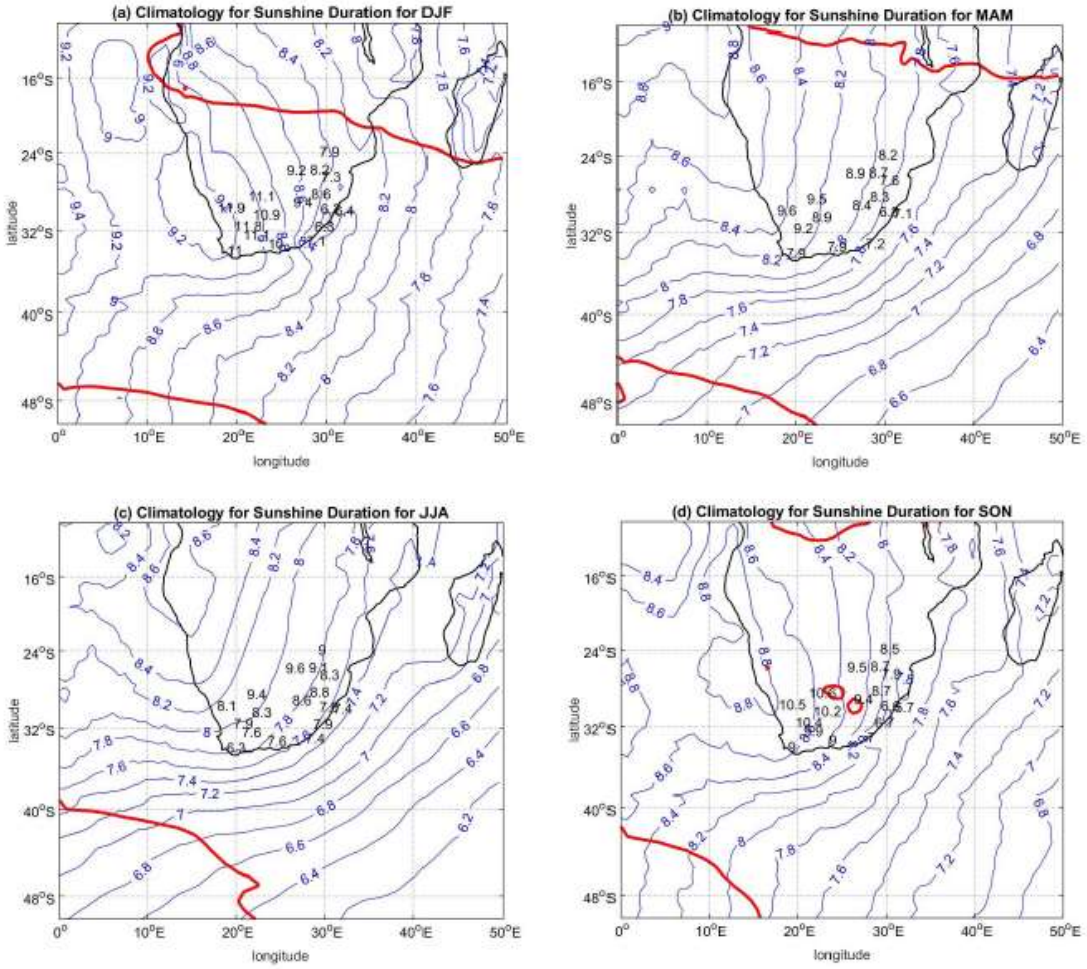

FIGURE 7 Sunshine duration (in hours) represented by the thin contours (ERA-Interim) and the values in black (SAWS observations). Regions where the mass flux is zero (thick contours) for (a) DJF, (b) MAM, (c) JJA and (d) SON

The frequency of major and truncated cloud bands is still high during transitional seasons. These bands define cloud cover over the north-western interior and southwards to the south eastern coasts during these seasons. Other cloud bands that define widespread cloud cover during the transitional seasons are the west coast and frontal bands, which result from an increase in frequency of westerly and easterly troughs over southern Africa. West coast troughs occur in

conjunction with active tropical convergence and are linked with west coast bands leading to widespread cloud cover over the central interior to the south western parts (Tyson and Preston-Whyte, 2000). The east coast troughs are associated with frontal brands and account for cloud cover over south eastern parts of South Africa (Tyson and Preston-Whyte, 2000). Because of the maximum subsidence that prevails over South Africa in JJA, least cloud cover is experienced and confined to the south western parts of the country (Figure 6c). Frontal activity is the main reason for cloud cover over the southern and south western parts of South Africa. The amount of sunshine duration exhibited at a location can be directly linked to cloud cover over the particular area, that is, areas of high sunshine duration coincide with areas of low cloud cover. This is quantified by strong negative correlations between the two (not shown), but also when comparing Figures 6 and 7. The abundance of sunshine as well as low values of cloud cover over South Africa is clearly evident in all seasons and seasonal variability is noticeable (Figure 7). In all seasons, the western interior of South Africa has the highest amount of sunshine duration and lowest cloud cover values. The eastern parts receive the least sunshine and highest amounts of cloud cover as shown in Kruger and Esterhuyse (2005) and this is consistent with the rainfall climatology (Tyson and Preston-Whyte, 2000). The effect of orography (Figure 1) is also evident over the higher lying areas, especially over Mpumalanga Province where high cloud cover and least sunshine are received.

3.4 Trends in mass flux, sunshine duration and total cloud cover

Linear trends of mass flux are displayed in Figure 8. During DJF, a statistically significant decrease in downwards mass flux is observed over the central and north eastern parts of South Africa. Simultaneously, an increase in downwards mass flux is established over the southern parts of South Africa (Figure 8a). In MAM (Figure 8b), a minimum decrease in downwards mass flux fashioned in a northwest to southeast directed band is evident over South Africa. This could indicate an increase in TTTs and the cloud bands that are associated with them. A tendency

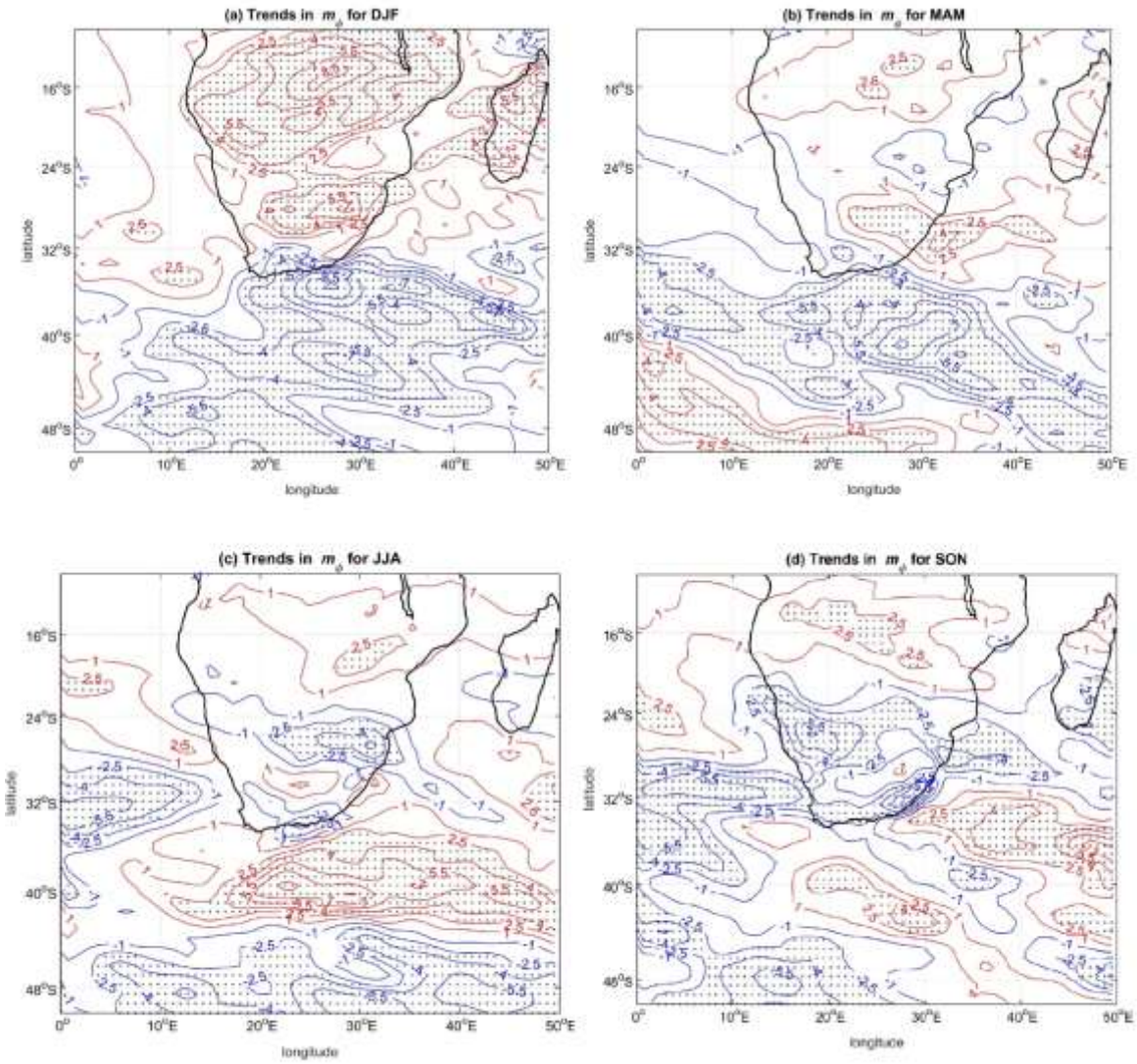

FIGURE 8 Trends in mass flux (kgm^{-2} s^{-1} $year^{-1}$) for (a) DJF, (b) MAM, (c) JJA and (d) SON. The contours represent positive and negative trends. The dotted regions represent 95% statistical significance greater than 0.5

towards an increase in the downwards mass flux is evident over the western, southern and north-eastern parts of the country. In JJA (Figure 8c), an increase in downwards mass flux is dominant over South Africa. However, there are some places over the interior showing a slight decrease in downwards mass flux.

For JJA the increase in downwards mass flux implies a strengthening of the Hadley over the country and could be as a result of an increase in the formation of midlevel-highs enhancing subsidence over the country (Engelbrecht et al., 2009). The maximum and statistically significant increase in downwards mass flux for most of South Africa is in SON (Figure 8d). It is only over Lesotho and some parts of northern KZN, where there is tendency towards a slight decrease in downwards mass flux in SON.

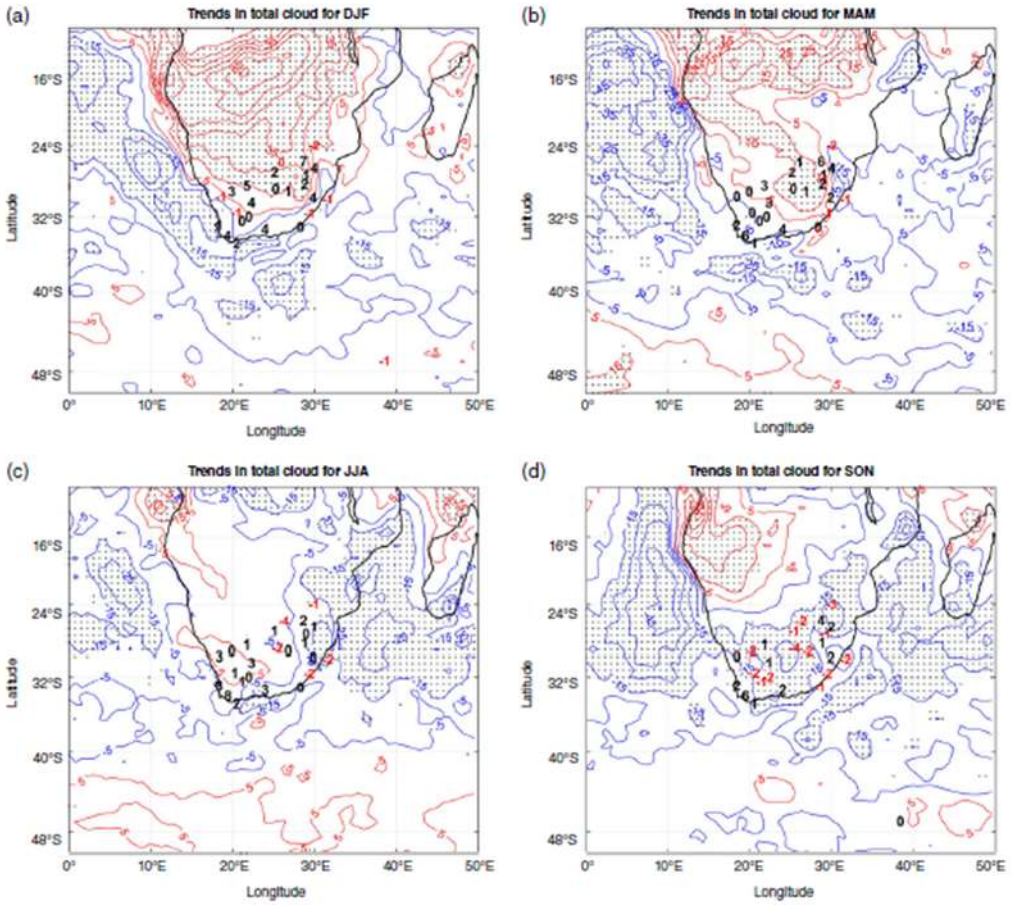

FIGURE 9 Same as in Figure 8 but for total cloud cover. Bold values represent trends for the SAWS station observation are represented as black values (positive trends) and red values (negative trends)

The ECMWF and the SAWS station data broadly indicate positive trends in total cloud cover during DJF and MAM (although there are stations showing an increasing trend) (see Figure 9a,b). In JJA, both observations show an increasing trend over the central interior and western parts of

the country (Figure 9c). Over the far eastern parts of South Africa, a decreasing trend is established from both data sets (Figure 9c). In SON, a decreasing trend dominates, based on both SAWS station data as well as the ECMWF data. The difference between the two data sets is evident over the south western parts in all seasons; SAWS station data advocate a decreasing trend while the ECMWF shows an increasing trend along that region.

Linear trends of sunshine duration are shown in Figure 10. Both ECMWF and SAWS observations broadly show statistically significant negative trends in sunshine duration for almost the entire country during DJF and MAM (Figure 10a, b). In JJA, the entire subcontinent records a decreasing trend of sunshine duration, with the exception of four SAWS stations that indicate an increasing trend (Figure 10c). Positive trends are evident during SON (Figure 10d) from both the ECMWF and SAWS observations. This is consistent with findings by Singh and Kruger (2017), which, although using point observations from weather stations across South Africa, use a similar period and found a general decrease in sunshine duration trends, mostly in DJF and MAM, while a maximum increase is recorded in SON. Trends between cloud cover and sunshine duration are largely consistent, with some areas of disagreement. Positive total cloud cover trends during DJF are found exactly where the negative sunshine duration trends are, except perhaps along coastal regions (Figure 10a).

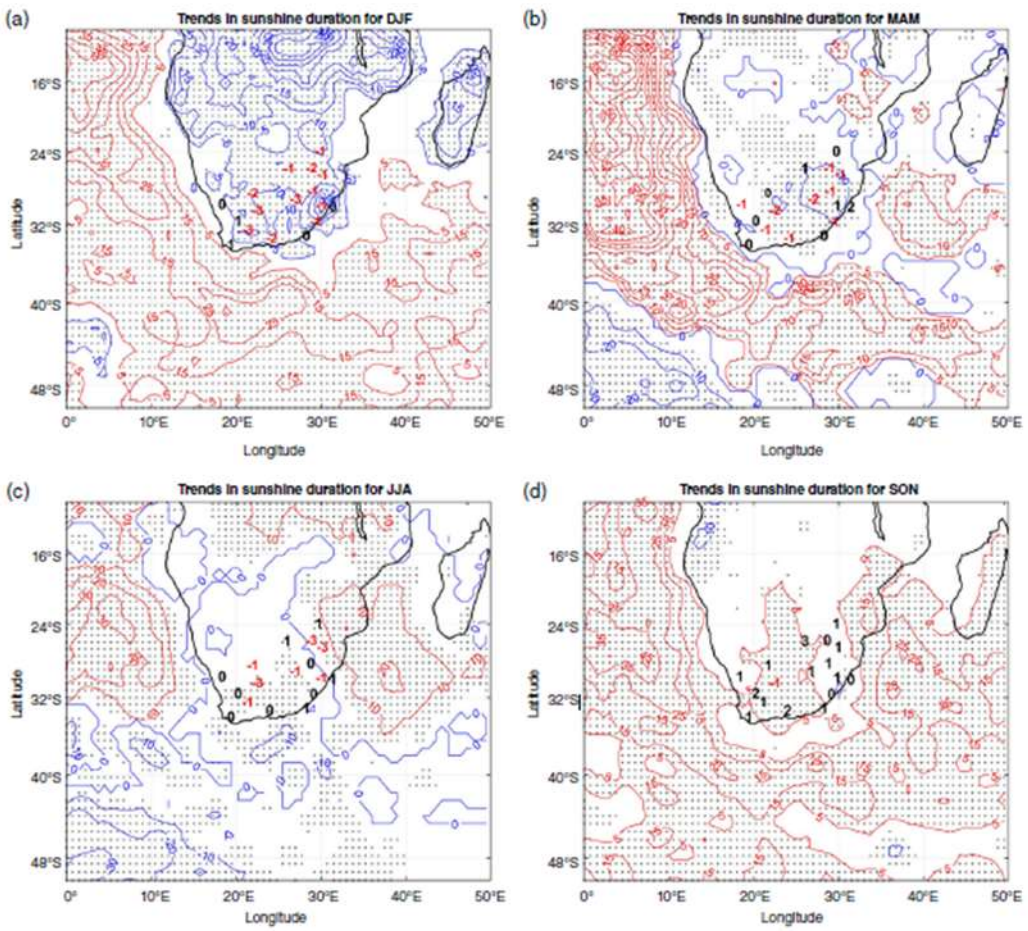

FIGURE 10 Same as in Figure 9 but for sunshine duration. Trends for the SAWS station observations are represented as red values (positive trends) and black values (negative trends)

In JJA, decreased cloud cover over the eastern regions and increased cloud cover over western regions is consistent with sunshine duration, which shows a tendency to decrease over western parts (although the spatial extent is relatively larger than the increase in total cloud cover) and increase over the eastern parts of South Africa (Figure 10c). Maximum decrease in cloud cover and maximum increase in sunshine duration is in SON (Figures 9d and 10d); this could imply that more opportunities for solar energy exist in SON. Changes in the Hadley circulation are in broad agreement with changes in total cloud cover and sunshine duration. Because the Hadley circulation is a fundamental process in the general circulation, we hypothesize here on the basis of these results that cloud cover and sunshine duration changes respond to changes in circulation.

4 CONCLUSIONS

This paper presents a combined climatology and trend analysis of the descending branch of the Hadley cell, cloud cover and sunshine duration over the subtropics and further over South Africa using zonally symmetric and asymmetric diagnostics, respectively. Although there is some form of consistency between the two diagnostics, a contrast has also been established. A weaker and more polewards Hadley is found in DJF, while a stronger and more equatorwards Hadley occurs in JJA. Consistently, the subtropical dry zones in the SH are located further southwards in DJF and further northwards in JJA. Associations between the Hadley cell, cloud cover and sunshine duration has been established from both diagnostics. Minimum total cloud cover, maximum sunshine duration, and the Hadley cell edges are located polewards in DJF, and equatorwards in JJA. Both diagnostics show maximum weakening of the Hadley in DJF. The maximum intensification of the subtropical Hadley, according to the zonally symmetric diagnostics is in JJA; however, the zonally asymmetric diagnostics indicate maximum intensification of the Hadley over South Africa to be in SON. The maximum intensification in SON coincides with a maximum decrease in cloud cover and increase in sunshine over South Africa.

Finally, apart from observing links between the Hadley cell, cloud cover and sunshine duration from the combined climatology and trends; the relationship between the Hadley cell and cloud cover was tested quantitatively using correlation coefficients. Results from the correlation coefficients suggest that cloud cover does not depend entirely on the Hadley cell. This is quite evident from the zonally asymmetric analysis, e.g. in DJF correlation was not established for almost the entire southern African region and mainly because cloud cover depends on weather systems that prevail over the country in summer. In JJA, cloudlessness over the interior of South Africa is informed by the Hadley cell and this could be the result of the correlation between the Hadley cell and cloud cover (although weak) over the interior of South Africa in JJA. It is evident from this study that the combined analysis of the Hadley cell, cloud cover and sunshine duration

may be obtained from both zonally symmetric and asymmetric analysis. However, using the zonally asymmetric diagnosis, it was established that different weather systems (e.g., TTTs and COLs) have a crucial role in this complex interplay. Thus, the next step will be to investigate the link between the Hadley cell and different climate systems that account for weather in southern Africa.

ACKNOWLEDGEMENTS

This work was financially supported by the National Research Foundation (NRF) Grant No. 102215. The authors are grateful to Dr Andries Kruger for his valuable input prior to the submission of this manuscript. Special thanks also go to the two anonymous reviewers for their contribution to improve the manuscript.

ORCID

D. D. Mahlobo https://orcid.org/0000-0003-2752-9062

S. Grab https://orcid.org/0000-0001-7678-1526

REFERENCES

Bergman, J.W. and Salby, M.L. (1997) The role of cloud diurnal variations in the time mean energy budget. Journal of Climate, 10, 1114–1124.

Bugaje, I.M. (2006) Renewable energy for sustainable development in Africa: a review. Renewable and Sustainable Energy Reviews, 10, 603–612.

Ceppi, P. and Hartmann, D.L. (2013) On the speed of the eddy-driven jet and the width of the Hadley cell in the Southern Hemisphere. Journal of Climate, 26, 3450–3465.

Cook, K.H. (2003) Role of continents in driving the Hadley cells. Journal of Atmospheric Sciences, 60, 957–976.

D'Abreton, P.C. and Tyson, P.D. (1995) Divergent and non-divergent water vapour transport over southern Africa during wet and dry conditions. Meteorology and Atmospheric Physics, 55, 47–59.

Dee, D.P., Uppala, S.M., Simmo, A.J., Berrisford, P., Poli, P., Kobayashi, S., Andrae, U., Balmaseda, M.A., Balsamo, G., Bauer, P., Bechtold, P., Beljaars, A.C.M., van de Berg, L., Bidlot, J., Bormann, N., Delsol, C., Dragani, R., Fuentes, M., Geer, A.J., Haimberger, L., Healy, S.B., Hersbach, H.,Hólm, E.V., Isaksen, L., Kållberg, P., Köhler, M., Matricardi, M., McNally, A.P., Monge-Sanz, B.M., Morcrette, J.-J., Park, B.-K., Peubey, C., de Rosnay,P., Tavolato, C., Thépaut, J.-N. and Vitart, F. (2011) The ERA-Interimreanalysis: configuration and performance of the data assimilation system.Quarterly Journal of the Royal Meteorological Society, 37, 553–597.

Engelbrecht, C.J. and Landman, W.A. (2014) Interannual rainfall variability over the Cape South Coast of South Africa linked to cut-off low associated rainfall. In: 30th Annual Conference of South African Society for AtmosphericSciences (SASAS), Potchefstroom, South Africa.

Engelbrecht, F.A., McGregor, J.L. and Engelbrecht, C.J. (2009) Dynamics of the conformal-cubic atmospheric model projected climate-change signal over southern Africa. International Journal of Climatology, 29, 1013–1033.

Engelbrecht, F.A., Landman, W.A., Engelbrecht, C.J., Landman, S., Bopape, M.M., Roux, B., McGregor, J.L. and Thatcher, M. (2011) Multi-scale climate modelling over southern Africa using a variable-resolution global model. Water SA, 37, 647–658.

Garfinkel, C.I., Waugh, D.W. and Polvani, L.M. (2015) Recent Hadley cell expansion: the role of internal atmospheric variability in reconciling modelled and observed trends. Geophysics Research Letter, 42(24), 824–831. https://doi.org/10.1002/2015GL066942.

Groisman, P.Y., Knight, R.W., Karl, T.R., Easterling, D.R., Sun, B. and Lawrimore, J.H. (2004) Contemporary changes of the hydrological cycle over the contiguous United States: trends derived from in situ observations. Journal of Hydrometeorology, 5, 64–85.

Hart, N.C.G., Reason, C.J.C. and Fauchereau, N. (2010) Tropical extratropical interactions over southern Africa: three cases of heavy summer season rainfall. Monthly Weather Review, 138, 2608–2623.

Holton, J.R. and Hakim, G.J. (2012) An Introduction to Dynamic Meteorology. Burlington, USA: Academic Press.

Johanson, C.M. and Fu, Q. (2009) Hadley cell widening: model simulations versus observations. Journal of Climate, 22, 2713–2725.

Kaggwa, M., Mutanga, S. and Simelane, T. (2011) Factors determining the affordability of renewable energy. A note for South Africa. Johannesburg, South Africa: AISA Policy Brief 65.

Kang, S.M. and Lu, J. (2012) Expansion of the Hadley cell under global warming: winter versus summer. Journal of Climate, 25, 8387–8393.

Keyser, D., Schmidt, B.D. and Duffy, D.G. (1989) A technique for representing three dimensional vertical circulations in baroclinic disturbances. Monthly Weather Review, 117, 2463–2494.

Kruger, A. (2007) Trends in cloud cover from 1960 to 2005 over South Africa. Water SA, 33, 603–608.

Kruger, A. and Esterhuyse, D. (2005) Climate of South Africa: Sunshine and Cloudiness, Vol. 35. Pretoria, South Africa: South African Weather Service.

Liepert, B.G. (2002) Observed reductions of surface solar radiation at sites in the United States and worldwide from 1961 to 1990. Geophysics Research Letter, 29(10), 1421. https://doi.org/10.1029/2002GL014910.

Loeb, N.G. and Schuster, G.L. (2008) An observational study of the relationship between cloud, aerosol and meteorology in broken low-level cloud conditions. Journal of Geophysical research, 113, D14214.

Lu, J., Vecchi, G.A. and Reichler, T. (2007) Expansion of the Hadley cell under global warming. Geophysics Research Letter, 34, L06805. https://doi.org/10.1029/2006GL028443.

Nguyen, H., Evans, A., Lucas, C., Smith, I. and Timbal, B. (2013) The Hadley circulation in reanalyses: climatology, variability, and change. Journal of Climate, 26, 3357–3376.

Polvani, L.M., Waugh, D.W., Correa, G.J.P. and Son, S.-W. (2011) Stratospheric ozone depletion:The main driver of the twentieth century atmospheric circulation changes in the Southern Hemisphere. Journal of Climate, 24, 795–812.

Power, H.C. and Mills, D.M. (2004) Trends in solar radiation over South Africa and Namibia during the period 1957–1997. AGU Spring Meeting Abstracts,

Ruiz-Arias, J.A., Pozo-Vázquez, D., Lara-Fanego, V., Santos-Alamillos, F.J. and Tovar-Pescador, J. (2011) A high-resolution topographic correction method for clear-sky solar irradiance derived with a numerical weather prediction model. Journal of Applied Meteorology and Climatology, 50, 2460–2472.

Schwendike, J., Govekar, P., Reeder, M.J., Wardle, R., Berry, G.J. and Jakob, C. (2014) Local partitioning of the overturning circulation in the Tropics and the connection to the Hadley and Walker circulations. Journal of Geophysical Research, 119, 1322–1339.

Schwendike, J., Berry, G.J., Reeder, M.J., Jakob, C., Govekar, P. and Wardle, R. (2015) Trends in the local Hadley and local Walker circulations. Journal of Geophysical Research, 120, 7599–7618.

Seidel, D.J. and Randel, W.J. (2007) Recent widening of the tropical belt: evidence from tropopause observations. Journal of Geophysical Research, 112, D020113.

Singh, J. and Kruger, A. (2017) Is the summer season losing potential for solar energy applications in South Africa. Journal of Energy in Southern Africa, 28, 52–60.

Solomon, S., Qin, D., Manning, M., Chen, Z., Marquis, M., Averyt, K.B., Tignor, M. and Miller, H.L. (2007) Summary for policymakers. In: Climate Change 2007: Synthesis Report. Contribution of Working Group I, II and III to the Fourth Assessment Report of the Intergovernmental Panel on Climate Change. Cambridge and New York, NY: Cambridge University Press.

Swarztrauber, P.N. (1974) The direct solution of the discrete Poisson equation on the surface of a sphere. Journal of Computational Physics, 15, 46–54.

Tselioudis, G., Lipat, B.R., Konsta, D., Grise, K.M. and Polvani, L.M. (2016) Midlatitude cloud shifts, their primary link to the Hadley cell, and their diverse radiative effects. Geophysics Research Letter, 43(9), 4594–4601.https://doi.org/10.1002/2016GL068242.

Tyson, P.D. and Preston-Whyte, R.A. (2000) The Weather and Climate of Southern Africa, 2nd edition. Cape Town, South Africa: Oxford University Press.

Wallace, J.M. and Hobbs, P.V. (2006) Atmospheric Science: An Introductory Survey. Amsterdam: Academic Press.

Wang, X. and Key, J.R. (2005) Arctic surface, cloud, and radiation properties based on the AVHRR polar pathfinder dataset. Part I: spatial and temporal characteristics. Journal of Climate, 18, 2558–2574.

Warren, G., Hahn, J., London, J., Chervin, M. and Jenne, L. (1986) Global distribution of total cloud cover and cloud type amounts over land. Boulder, Colorado:NCAR technical note NCAR/TN273+STR.

Warren, S.G., Eastman, R.M. and Hahn, C.J. (2007) A Survey of changes in cloud cover and cloud types over land from surface observations, 1971–96. Journal of Climate, 24, 795–812.

APPENDIX A: DERIVATION OF THE ZONALLY SYMMETRY Hadley cell USING THE ZONALLY AVERAGED MASS-STREAM FUNCTION

The strength and structure of the Hadley cell can be quantified using the zonally averaged stream function, given by the following motivation.

In the isobaric vertical coordinate system, the spherical version of the continuity equation is given by

$$\frac{1}{acos\phi}\frac{\partial u}{\partial \lambda}+\frac{1}{acos\phi}\frac{\partial \omega}{\partial p}(vcos\phi)+\frac{\partial \omega}{\partial p}=0 \qquad \text{(A1)}$$

where u and v are the zonal meridional components of the divergent ageostrophic flow, espectively, ω the vertical component of the velocity, a is the radius of the earth, λ is the longitude and ϕ is the latitude. The zonally averaged Equation (A1) reduces to its two-dimensional version, given by

$$\frac{1\partial \bar{v}}{a\partial \phi}+\frac{\partial \bar{\omega}}{\partial p}=0 \qquad \text{(A2)}$$

The overbar in Equation (A2) represents zonally averaged fields. Equation (2) represents non-divergent two dimensional flow on the meridional plane, and so it can be represented in terms of a streamfunction (ψ), so that the zonally averaged meridional and vertical components of the wind fields may written as

$$\bar{v}=\frac{g\partial \Psi}{2\pi cos\phi \partial p} \qquad \text{(A3)}$$

$$\bar{\omega}=-\frac{g\partial \Psi}{2\pi a^2 cos\phi d\phi} \qquad \text{(A4)}$$

Because both components in Equations (A3) and (A4) satisfy the continuity equation described in Equation (A2), either one of them can be used to solve for the stream function ψ by integrating the vertical and meridional directions, respectively. However, most studies (e.g., Polvani et al., 2011) make use of the expression involving $\bar{v}$ because the meridional velocity is more directly and more accurately observed than $\bar{\omega}$.

APPENDIX B: DERIVATION OF THE ZONALLY ASYMMETRIC Hadley cell USING A VARIATION OF THE STREAM FUNCTION VECTOR METHOD

In this section we follow Schwendike et al. (2014) to outline the approach they took to partition the isobaric continuity equation (see Equation (A1)). On each isobaric surface, the divergent, irrotational flow in Equation (A1) may be written in terms of a velocity potential χ, such that

$u = \frac{1}{a\cos\phi}\frac{\partial \chi}{\partial \lambda}$ and

$$v = \frac{1}{a\cos\phi}\frac{\partial}{\partial \phi}(\chi\cos\phi) \qquad \text{(B1)}$$

Since $\nabla \times \nabla\chi = 0$, Le

$$\chi \equiv \frac{\partial \mu}{\partial p} \qquad \text{(B2)}$$

where μ is a potential function, and then combine this with A0 to produce a Poison's equation in μ, that is,

$$\frac{1}{a^2\cos^2\phi}\frac{\partial^2 \mu}{\partial \lambda^2} + \frac{1}{a^2\cos\phi}\frac{\partial}{\partial \phi}(\sin\phi)\frac{\partial \mu}{\partial \partial \phi} = -\omega \qquad \text{(B3)}$$

which is solved numerically, given suitable boundary conditions as discussed in section 2.2.2.

Now define a vector stream function $\vec{\Psi}$ (here the over arrow indicates that this quantity is a vector), such that

$\psi_\lambda = -\frac{1}{a\cos\phi}\frac{\partial \mu}{\partial \lambda}$ and

$$\psi_\phi = -\frac{1}{a}\frac{\partial \mu}{\partial \phi} \qquad \text{(B4)}$$

and taking the divergence of $\vec{\Psi}$ (and using Equation (B3), we obtain

$$\frac{1}{acos\phi}\frac{\partial\psi_\lambda}{\partial\lambda}+\frac{1}{acos\phi}\frac{\partial}{\partial\phi}\left(\psi_\phi cos\right)=\omega \qquad \text{(B5)}$$

Clearly, from Equation (B5), vertical motion ω is partitioned into two orthogonal directions so

$$\omega_\lambda cos\phi=\frac{1}{a}\frac{\partial\psi_\lambda}{\partial\lambda} \qquad \text{(B6)}$$

$$\omega_\phi cos\phi=\frac{1}{a}\frac{\partial}{\partial\phi}\left(\psi_\phi cos\phi\right) \qquad \text{(B7)}$$

With $\omega=\ \omega_\lambda+\ \omega_\phi$

It follows then from Equations (B1) and (B2) that the zonal component of the ageostrophic flow may be written in terms of zonal component of the ψ vector:

$$u=\frac{1}{acos\phi}\frac{\partial}{\partial\lambda}\left(\frac{\partial\mu}{\partial p}\right)=\frac{\partial}{\partial p}\left(\frac{1}{acos\phi}\frac{\partial\mu}{\partial\lambda}\right)=-\frac{\partial\psi_\lambda}{\partial p} \qquad \text{(B8)}$$

Similarly, the meridional component of the ageostrophic flow may be written in terms of meridional component of the ψ vector as follows:

$$v=-\frac{\partial\psi_\phi}{\partial p} \qquad \text{(B9)}$$

Using Equations (B6) and (B8) and the fact that partial derivatives are interchangeable, we have

$$\frac{1}{a}\frac{\partial u}{\partial\lambda}+\frac{\partial}{\partial p}(\omega_\lambda cos\phi)=0 \qquad \text{(B10)}$$

Similarly,

$$\frac{1}{a}\frac{\partial}{\partial\phi}(vcos\phi)+\frac{\partial}{\partial p}\left(\omega_\phi cos\phi\right)=0 \qquad \text{(B11)}$$